Nutrition and Cancer

ISSN: 0163-5581 (Print) 1532-7914 (Online) Journal homepage: www.tandfonline.com/journals/hnuc20

Carvacrol Induces Reactive Oxygen Species (ROS)-mediated Apoptosis Along with Cell Cycle Arrest at G_0/G_1 in Human Prostate Cancer Cells

Fahad Khan, Imran Khan, Arshi Farooqui & Irfan A. Ansari

To cite this article: Fahad Khan, Imran Khan, Arshi Farooqui & Irfan A. Ansari (2017) Carvacrol Induces Reactive Oxygen Species (ROS)-mediated Apoptosis Along with Cell Cycle Arrest at G_0/G_1 in Human Prostate Cancer Cells, Nutrition and Cancer, 69:7, 1075-1087, DOI: 10.1080/01635581.2017.1359321

To link to this article: https://doi.org/10.1080/01635581.2017.1359321

Published online: 05 Sep 2017.

NUTRITION AND CANCER
2017, VOL. 69, NO. 7, 1075–1087
https://doi.org/10.1080/01635581.2017.1359321

Taylor & Francis
Taylor & Francis Group

Carvacrol Induces Reactive Oxygen Species (ROS)-mediated Apoptosis Along with Cell Cycle Arrest at G_0/G_1 in Human Prostate Cancer Cells

Fahad Khan, Imran Khan, Arshi Farooqui, and Irfan A. Ansari

Department of Biosciences, Integral University, Lucknow, Uttar Pradesh, India

ABSTRACT

Carvacrol, a major monoterpenoid phenol from *Origanum* and *Thymus* species, has been shown to exhibit antiproliferative and anticancer properties in a few recent studies. Nevertheless, detailed mechanism of the action of this compound in prostate cancer has not been elucidated yet. Therefore, in the current study, we examined the anticancer activity and mechanism of the action of carvacrol against human prostate cancer cells. It was found that the treatment of DU145 cells with carvacrol decreased cell viability in a concentration and time-dependent manner. The antiproliferative action of carvacrol leads to induction of apoptosis as confirmed by nuclear condensation, Annexin V-FITC/PI positive cells, and caspase-3 activation. In addition, carvacrol augmented reactive oxygen species generation and disruption in the mitochondrial membrane potential which has not been reported in the previous studies of carvacrol with prostate cancer. Moreover, carvacrol-induced apoptosis of prostate cancer cells was also accompanied by significant amount of growth arrest at the G_0/G_1 phase of the cell cycle which has also not been documented previously. To sum up, this study has established that carvacrol could be a promising chemotherapeutic agent and could have a direct practical implication and translational relevance to prostate cancer patients as *Origanum* consumption may retard prostate cancer progression.

ARTICLE HISTORY
Received 17 December 2016
Accepted 26 June 2017

Introduction

Prostate cancer represents the second most prevalent cancer in males worldwide and is a major cause of morbidity and mortality. Recent statistical reports show that approximately 1.1 million men worldwide (15% of the total) were diagnosed with prostate cancer in 2012,with almost 70% of the cases (759,000) occurring in more developed regions (1). With an estimated 307,000 deaths in 2012, prostate cancer is the fifth leading cause of death from cancer in men (6.6% of the total men deaths) (1). Case fatality rate in low-income countries (78.6%) is 3.5 times that of high-income countries (22.5%) (2).

Although prostate cancer rates in India are lower than those seen in Western countries, increasing life expectancy and adoption of newer lifestyles are bringing about an increase in these rates. It is the third leading cause of cancer-related death in Indian male, posing a major health problem (3). The most recent Population-Based Cancer Registries (PBCRs) of different cities for the time period 2008–2011 shows that prostate cancer is the second leading cancer among Indian males with highest cancer incidence rates in metro cities like Delhi, Mumbai, Kolkata, Chennai, Bangalore, and Pune (4). The incidence rates of prostate cancer are constantly and rapidly increasing in all the PBRCs and the projected cases at all-India level for the year 2020 was estimated to be 30,185 (5).

Despite advances in the treatment of prostate cancer, therapies for recurrent or persistent cancers and alternative treatment options with low toxicity are inadequate. In the absence of satisfactory treatment options, chemoprevention could be an effective approach to reduce the incidence of prostate cancer. Therefore, much research has been focused on the identification of chemopreventive agents with least side effects as an additional approach for the management of prostate cancer. For a variety of reasons, the most important of which is human acceptance, chemoprevention through dietary intervention has been regarded as a more practical approach (6,7). In the past few decades, natural products have been identified as promising agents for cancer prevention and treatment based on their ability to attack multiple molecular targets and cellular signaling pathways (8). Many such naturally occurring phytochemicals for

CONTACT Irfan A. Ansari iaansari@iul.ac.in; ahmadirfan.amu@gmail.com Department of Biosciences, Integral University, Lucknow 226026, Uttar Pradesh, India.

Color versions of one or more of the figures in this article can be found online at www.tandfonline.com/hnuc.

chemoprevention of prostate cancer are being evaluated in cell culture and in animal model systems (9). It is noteworthy that some of these agents have been shown to be promising in prostate cancer patients (10).

Carvacrol [2-methyl-5-(1-methylethyl)-phenol], is a major monoterpenoid phenol present in the essential oil from the plants of family Lamiaceae including *Origanum, Thymus, Satureja*, and *Carum* species. The highest naturally occurring carvacrol content (80%) has been found in the oil from *O. vulgare*. The essential oil from the above plant species has been used as a safe food additive in beverages, baked goods, and sweets in the food industry from a long time (11). Carvacrol has been shown to exhibit a broad range of therapeutic effects, including anti-oxidant, anti-inflammatory, anti-angiogenic, and anti-tumor activity (12–21). It has gained considerable attention recently because of its potential chemopreventive properties. In a few recent studies, carvacrol has been shown to have antiproliferative and anticancer activities against human metastatic breast cancer MDA-MB231 cells, chronic myeloid leukemia K562 cells, non-small cell lung cancer A549 cells, and murine B16 melanoma cells (22–28). Nevertheless, the detailed underlying mechanism of the action of this compound in prostate cancer has not been elucidated yet. Therefore, aim of the present study was to explore the anticancer potential and underlying mechanism of the action of carvacrol against prostate cancer cells.

Materials and Methods

Cell Lines and Reagents

Dulbecco's modified eagle medium (DMEM), modified essential medium (MEM), fetal bovine serum (FBS), Trypan blue and 3-(4,5-dimethylthiazol-2-yl)-2,5-diphenyltetrazolium-bromide (MTT) and other chemicals were purchased from Himedia India, Ltd., Mumbai, India. Carvacrol, 2′,7′-dichlorodihydrofluorescein diacetate (DCFH-DA), DAPI (4′,6-diamidino-2-phenylindole), propidium iodide (PI) solution, and Rhodamine123 (Rh123) were purchased from Sigma (St. Louis,MO, USA). Annexin V-FITC Apoptosis Detection Kit was obtained from BD Bioscience, PharMingen (San Diego, CA, USA).

Cell Culture

Human prostate cancer DU145 and normal mouse macrophage J774A.1cells were obtained from Cell Repository, National Centre for Cell Sciences, Pune, India. DU145 cells were cultured in MEM and J774A.1 cells were cultured in DMEM supplemented with 100 μg/ml penicillin/streptomycin/amphotericin B (Himedia, India, Ltd., Mumbai, India) and 10% heat-inactivated FBS. The cells were incubated at 37°C in a humidified atmosphere containing 5% CO_2.

Cell Viability Assay

The MTT assay was used to assess the effect of carvacrol on DU145 prostate cancer cells as described previously (29). Exponentially growing DU145 cells (5×10^3 cells/well) were seeded in a 96-well culture plate and allowed to attach overnight and further treated with 0, 10, 25, 50, 100, 250, and 500 μM of carvacrol for 24 and 48 h. At the end of the drug treatment, 10 μl of MTT (5 mg/ml) was added to each well and the plates were incubated for another 4 h at 37°C. 100 μl of dimethyl sulfoxide was added to each well and thoroughly mixed to dissolve the purple crystals. The absorbance of each well was measured on a microplate reader (Bio-Rad, USA) at 490-nm wavelength and the cell survival was expressed as the percentage (%) over the untreated control.

Trypan Blue Dye Exclusion Assay

Carvacrol-induced cytotoxicity in DU145 cells was also determined by trypan blue dye exclusion cell death assay, as described previously (30). Briefly, 5×10^4 cells were treated with or without carvacrol (0, 10, 25, 50, 100, 250, and 500 μM) for 24 and 48 h. Thereafter, cells were harvested, stained with 0.25% trypan blue dye, and the cells that had taken up the dye were counted under a microscope using a hemocytometer. The carvacrol-induced cell death was expressed as the percentage of dead cells in each treatment group from three independent experiments.

Morphological Analysis by Phase Contrast Microscopy

Morphological changes associated with carvacrol-treated DU145 and J774A.1 cells were analyzed as described previously (31). The cells were cultured in a 96-well plate at a density of 5×10^3 cells per well. The cells were cultured overnight and then replenished with fresh medium containing various concentrations (0, 10, 25, 50, 100, 250, and 500 μM) of carvacrol for 24 and 48 h. After incubation, cellular morphology of treated cells and untreated control were observed under inverted phase contrast microscope (Labomed, U.S.A).

Detection of Nuclear Condensation by DAPI staining

Morphological changes associated with nuclear condensation in DU145 cells were also detected by DAPI

staining as described previously (32). Briefly, DU145 cells (5×10^4 cells/well) were placed in a 12-well plate for 24 h. The cells were treated with various doses of carvacrol (0, 25, 50, 100, 250, and 500 μM) for 12 h and then washed with cold PBS. Finally, the cells were fixed in methanol for 10 min. Subsequently, cells were permeabilized with permeabilizing buffer (0.25% Triton X-100) and stained with DAPI. Then, the cells were examined under an inverted fluorescence microscope (Nikon ECLIPSE Ti-S, Japan).

Determination of Nuclear Morphology by Hoechst 33342 Staining

Morphological changes associated with apoptosis in DU145 cells were further detected by Hoechst 33342 staining (33). Briefly, cells (5×10^4 cells/well) were seeded in a 12-well plate and treated with different concentrations of carvacrol (0, 25, 50, 100, 250, and 500 μM) for 12 h. Cells were washed by PBS, and then stained with 5 μg/ml Hoechst 33342 for 10 min at 37°C in a humidified dark chamber. Then nuclear morphology of cells was examined under an inverted fluorescence microscopy (Nikon ECLIPSE Ti-S, Japan).

Annexin V-FITC/PI Assay to Analyze Apoptosis

Apoptosis was analyzed using the annexin V/PI apoptosis kit (BD Biosciences, San Diego, CA, USA) according to the manufacturer's recommendations. Briefly, DU145 cells were first seeded into 60-mm culture dishes and treated with carvacrol (0, 25, 50, 100, and 250 μM) for 24 h. The cells were washed twice with cold PBS and then resuspended in 1X binding buffer at a concentration of 1×10^6 cells/ml. 100 μl of the cell suspension (1×10^5 cells) was transferred to a 5-ml culture tube. Then, 5 μl of FITC-Annexin V conjugate and 5 μl of PI were added to the cell suspension. After incubation for 15 min in the dark at room temperature (25°C), 400 μL of the 1x binding buffer was added to the cell suspension. The stained cells were then immediately analyzed on a FACS Calibur flow cytometer (BD Biosciences, San Diego, CA, USA).

Analysis of Caspase-3 Activity

The caspase-3 activity was assayed using Caspase-3 Colorimetric Assay Kit (BioVision, USA). Approximately 3×10^6 cells, untreated and treated, (0, 25, 50, 100, and 250 μM) were lysed in 50 μl of chilled cell lysis buffer and incubated on ice for 10 min. The cell lysate was centrifuged for 1 min at 10,000 $\times$ g. The supernatant of the cell lysate was collected and put on ice for immediate assay. The cell lysate was properly diluted with 50 μl of cell lysis buffer after protein quantification. The lysate (50 μl) was aliquoted into 96-well plate and 50 μl of reaction buffer, containing 10 mM DTT, was added to each sample. After that, 5 μl of the 4 mM DEVD-*p* NA substrate was added in each well and incubated at 37°C for 1 h. Absorbance was then read at 405 nm in a microtiter plate reader. Percent (%) increase in caspase-3 activity was determined by comparing these results with the level of the uninduced control.

Analysis of the Effect of Caspase-3 Inhibitor (Z-DEVD-FMK)

To characterize the cytotoxicity of carvacrol, DU145 cells were pretreated with 50 μM of Z-DEVD-FMK (a caspase-3 inhibitor) for 2 h and then treated with carvacrol at the indicated concentrations for 24 h. The cell viability was determined using the MTT assay as described above.

Measurement of Intracellular ROS Level

The intracellular reactive oxygen species (ROS) level was measured by DCFH-DA method as described elsewhere (34,35). It is based on the ROS-induced formation of the highly fluorescent product 2′,7′-dichlorofluorescein (DCF) from the non-fluorescent dye 2′,7′-dichlorofluorescin diacetate (DCFH-DA). Briefly, DU145 cells were seeded in a 12-well plate at a density of 5×10^4 cells per well and incubated for 24 h at 37°C. Following treatment with carvacrol (0, 25, 50, 100, 250, and 500 μM) for 12 h, the cells were incubated with 10 μM DCFH-DA for 30 min at 37°C. After the removal of excessive DCFH-DA by washing, images were captured by using an inverted fluorescence microscope (Nikon ECLIPSE Ti-S, Japan).

For quantitative ROS analysis, cells (1×10^4/well) were re-seeded in 96-well black bottom culture plate and allowed to adhere for 24 h in a CO_2 incubator at 37°C. DU145 cells were treated with different concentrations of carvacrol as mentioned for 12 h. Cells were further incubated with DCFH-DA (10 μM) for 30 min at 37°C. Fluorescence intensity was measured by a multiwall microplate reader (Synergy H1 Hybrid Multi-Mode Microplate Reader, BioTek, USA) at an excitation wavelength of 485 nm and emission wavelength of 528 nm. Values were expressed as the percentage of fluorescence intensity relative to the control wells.

Analysis of the Effect of a ROS Inhibitor, N-Acetyl-L-Cysteine (NAC)

To confirm the generation of intracellular ROS in carvacrol-treated prostate cancer cells, the cells were

pretreated with 10 mM NAC for 2 h and then treated with carvacrol (0, 25, 50, 100, 250, and 500 μM) for 12 h. Cells were then washed with PBS and incubated with 10 μM DCFH-DA for 30 min at 37°C. Fluorescence intensity was measured by a multiwall microplate reader (Synergy H1 Hybrid Multi-Mode Microplate Reader, BioTek, USA) at an excitation wavelength of 485 nm and emission wavelength of 528 nm. To further investigate the role of ROS in carvacrol-induced apoptosis in prostate cancer cells, we examined the effect of carvacrol on DU-145 cells, in the presence of NAC (10 mM), a specific ROS scavenger, using the MTT assay.

Detection of Mitochondrial Membrane Potential ($\Delta\Psi m$) by Rh123 Staining

The effect of carvacrol on mitochondrial transmembrane potential was evaluated using rhodamine123 (Rh123) as described previously (36). Briefly, DU145 cells (2×10^5 cells/well) were cultured in a 12-well plate and allowed to attach overnight. Cells were treated with carvacrol at different concentrations (0, 25, 50, 100, 250, and 500 μM) for 12 h. After washing, cells were incubated with Rh123 (5 μg/ml) for 30 min in the dark. Then the cells were photographed using an inverted fluorescence microscope (Nikon ECLIPSE Ti-S, Japan).

Cell Cycle Analysis

Cell cycle analysis of carvacrol-treated DU145 cells was performed with the intercalating DNA fluorochrome, PI as described earlier (31,37). Briefly, DU145 cells (5×10^5 cells) were cultured in a 60-mm tissue culture dish for 24 h at 37°C and 5% CO_2 and treated with carvacrol (0, 25, 50, 100, and 250 μM) for another 24 h. Cells were harvested, washed with PBS by centrifugation at 600 g for 5 min and treated with RNase A (200 μg/ml) for 30 min at 37°C. Subsequently, cells were fixed with ice cold 70% ethanol overnight at −20°C and finally, stained with PI (25 μg/ml) for 15 min at room temperature. Cell cycle analysis was performed using a flow cytometer (Becton Dickinson FACS Calibur, San Jose, CA).

Statistical Analysis

The data were presented as the mean ± SEM of three independent experiments performed in triplicates. Statistical analysis was performed by one-way ANOVA using Dunnett's multiple comparison test and also by two-tailed, paired Student's *t*-test ($^{*}P < 0.01$, $^{**}P < 0.001$, $^{***}P < 0.0001$ represent significant difference compared with control).

Results

Carvacrol Did Not Exert Significant Effect on Normal Macrophage J774A.1 Cells

To find out the experimental doses and cytotoxicity of carvacrol, MTT assay and assessment of cell morphology were performed on normal mouse macrophage J774A.1 cells. Cell viability data showed that after 24 h of treatment, percent cell viability of normal cells as compared to control was 98.20%, 95.79%, 94.93%, 94.73%, and 90.47% at 10, 25, 50, 100, and 250 μM dose of carvacrol, respectively; which were found to be statistically insignificant. Similarly, we did not find any significant effect on cell viability of macrophages after 48 h of carvacrol treatment with 10, 25, 50, 100, 250, and 500 μM concentrations. However, a significant reduction in cell viability (87.10% and 86.27%) was observed at 500 μM of carvacrol after 24 and 48 h of treatment (Fig. 1A). Furthermore, morphological study suggested that after 24 and 48 h of treatment, higher concentration of carvacrol (500 μM) altered cell morphology and induced cell death in normal macrophages. However, 10, 25, 50, 100, and 250 μM of carvacrol at the above-mentioned time periods did not exert significant effect on cell morphology (data not shown). Thus, the results of this study have established that carvacrol did not show considerable cytotoxic effect in normal cells.

Carvacrol Inhibited Proliferation of Prostate Cancer DU145 Cells

The cytotoxic effect of carvacrol on DU145 prostate cancer cells was determined by treating cells with varying concentrations of the carvacrol (0, 10, 25, 50, 100, 250, and 500 μM) for 24 and 48 h. The data indicated that treatment of cells with different concentrations of carvacrol resulted in significant inhibition of cell viability as compared to controls (Fig. 1B). Carvacrol inhibited proliferation of DU145 cells in a concentration and time-dependent manner with median inhibitory concentrations (IC_{50}) of around 84.39 μM and 42.06 μM, for 24 h and 48 h respectively. The results showed that after 24 h of treatment at 25, 50, and 100 μM carvacrol, cell viability of DU145 cells significantly reduced to around 79.42%, 59.48%, and 46.85%, respectively as compared to control, which further dropped to 15.63% and 11.70% at 250 and 500 μM, respectively. Similarly, after 48 h of treatment at 25, 50, 100, 250, and 500 μM carvacrol, viability of DU145 cells reduced to 77.09%, 51.92%, 29.36%, 11.91%, and 9.89%, respectively as compared to control (Fig. 1B). Carvacrol could not exert any significant cytotoxic effect on prostate cancer cells at the dose

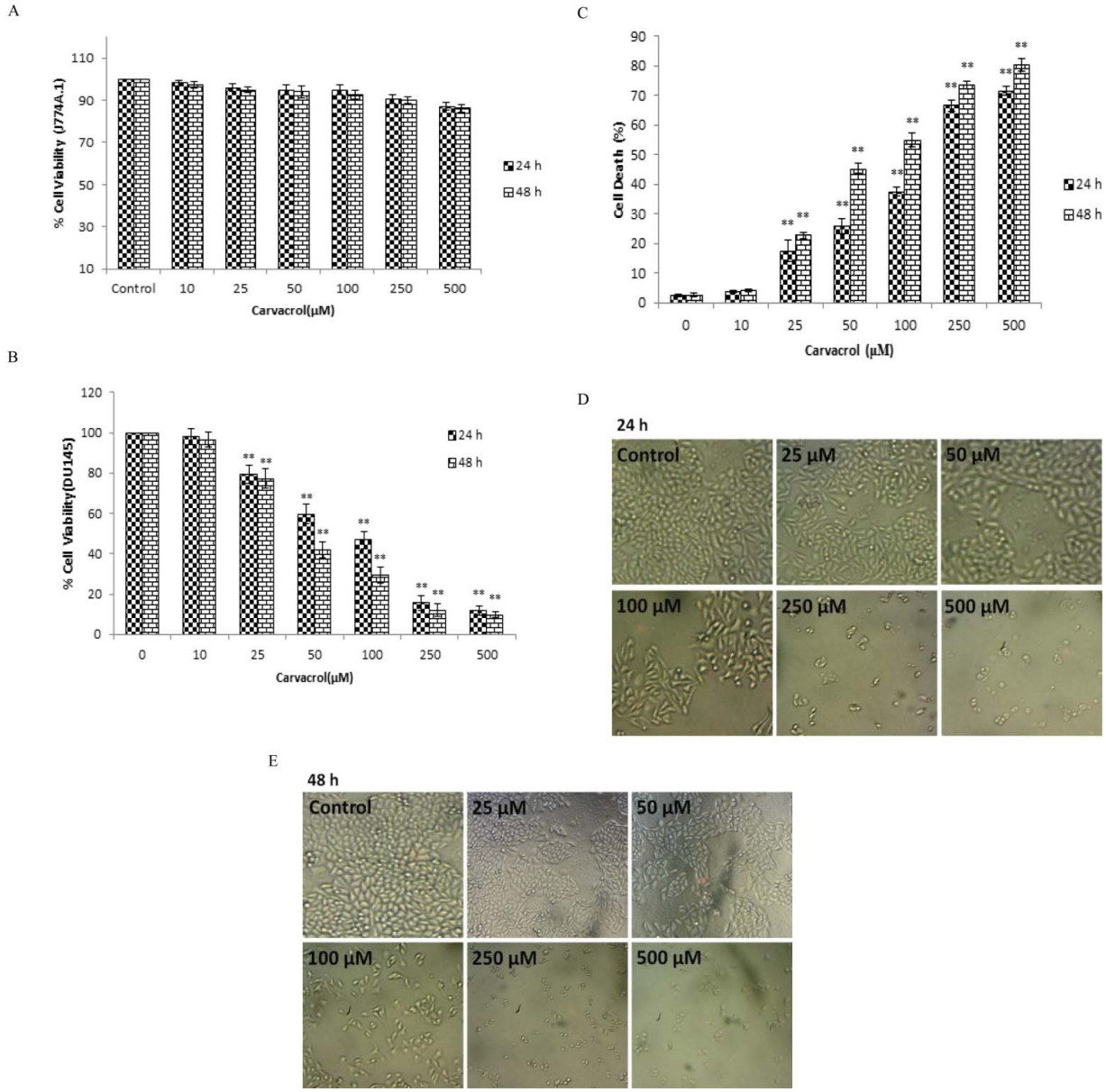

Figure 1. Dose and time-dependent effect of carvacrol on normal J774.1 cells and human prostate cancer DU145 cell line. A: Percent cell viability of normal J774A.1 cells treated with different doses of carvacrol (0–500 μM) for 24 and 48 h assessed by MTT assay. B: Percent cell viability of DU145 cells treated with different doses of carvacrol (0–500 μM) for 24 and 48 h assessed by MTT assay. C: Percent cell death of DU145 cells treated with different doses of carvacrol (0–500 μM) for 24 and 48 h assessed by trypan blue dye exclusion assay The results represented are the mean ± SEM of three independent experiments performed in triplicate ($^{*}P < 0.01$, $^{**}P < 0.001$, $^{***}P < 0.0001$ represent significant difference compared with control). D and E: Phase-contrast photomicrograph of DU145 cells treated with either vehicle control or different doses of carvacrol (0–500 μM) for 24 and 48 h. Images shown are representative of three independent experiments.

10 μM after 24 and 48 h of treatment, which was evident by the cell viability of 98.07% and 96.60% at respective time periods.

In an additional experiment, we determined the cytotoxic effect of carvacrol by trypan blue exclusion assay. Treatment of DU145 cells with carvacrol, at the doses of 0, 10, 25, 50, 100, 250, and 500 μM for 24 and 48 h, resulted in significant cell death (Fig. 1C). The results showed that, when compared to control, treatment of DU145 cells with carvacrol for 24 h resulted in significant amount of cell death of around 17.44%, 25.88%, 37.66%, 66.68%, and 71.62% at 25, 50, 100, 250, and 500 μM, respectively, which further increased to around 22.81%, 45.29%, 55.08%, 73.45%, and 80.52% after 48 h of treatment at 25, 50, 100, 250, and 500 μM, respectively. Moreover, carvacrol did not show any significant cytotoxic effect on prostate cancer cells at the dose 10 μM after 24 and

48 h of treatment, which was evident by the cell death of around 3.63% and 4.37% at respective time periods. Thus, the above results have established that carvacrol could induce substantial cytotoxic effects in human prostate cancer cells without having significant cytotoxic effect on normal cells.

Carvacrol-Induced Morphological Changes in Prostate Cancer Cells

Phase-contrast microscopic analysis of carvacrol-treated DU145 revealed significant morphological changes in prostate cancer cells treated with different concentrations of carvacrol (0, 25, 50, 100, 250, and 500 μM) as compared to control, which include retraction of cellular processes and cell shrinkage (Fig. 1D and E). These morphological changes in DU145 cells were more pronounced with increase in carvacrol concentration. In contrast, the control cells were well spread with a flattened morphology.

Carvacrol-Induced Nuclear Condensation Along with Apoptosis in DU145 Cells

DAPI and Hoechst 33342 staining was performed to characterize whether carvacrol-mediated inhibition of cell viability in prostate cancer cells is a result of induction of apoptosis. After treatment with carvacrol (0, 25, 50, 100, 250, and 500 μM) for 24 h, marked morphological changes in prostate cancer DU145 cells were observed. Condensed and fragmented nuclei were regarded as apoptotic cells. As evident from fluorescence micrographs, carvacrol induced nuclear condensation and fragmentation in DU145 cells in a dose-dependent manner as indicated by the arrow (Fig. 2A). The control cells exhibited normal cell

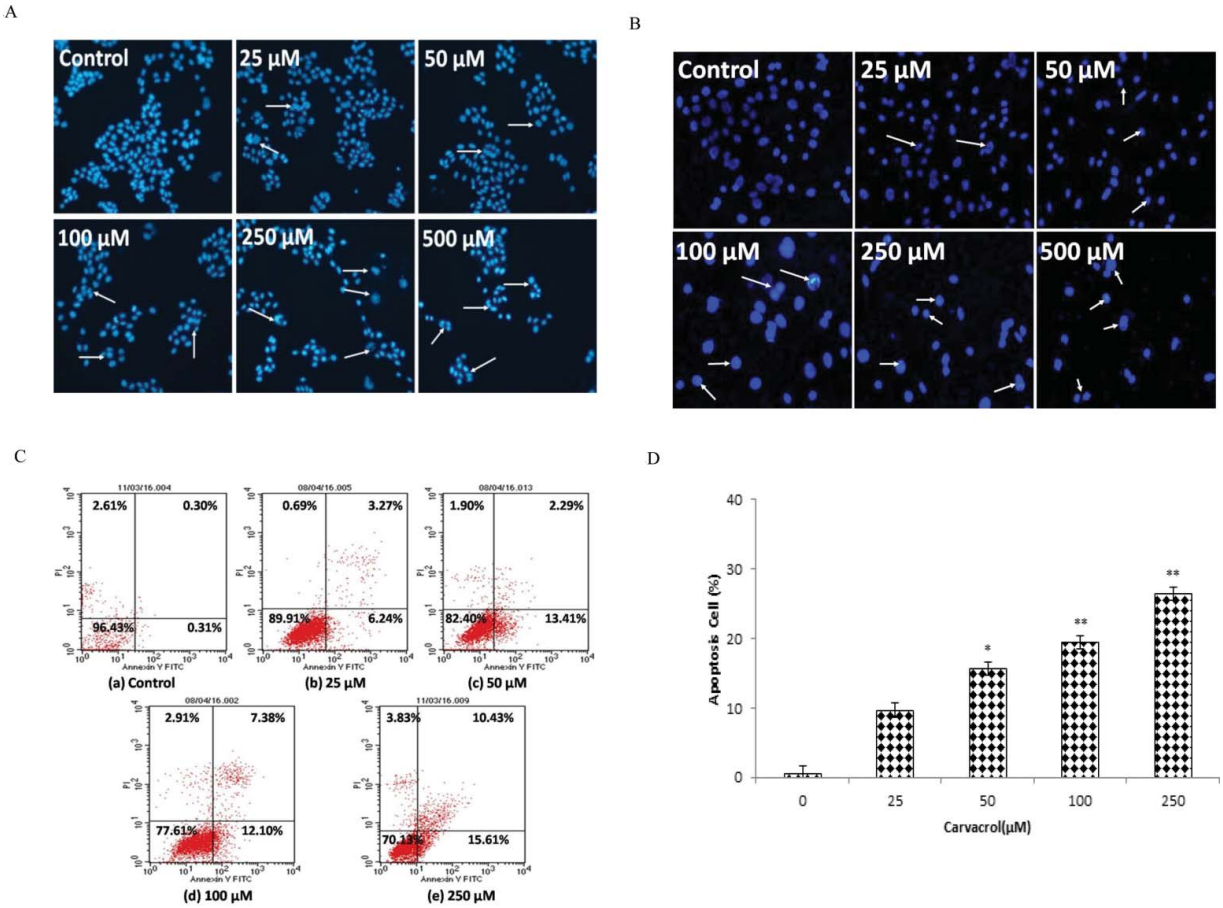

Figure 2. Carvacrol induced apoptosis in human prostate cancer DU145 cells. A: Nuclear morphology of (A) DAPI and (B) Hoechst-stained nuclei of DU145 cells treated with varying concentrations of carvacrol (0–500 μM) for 24 h analyzed by fluorescence microscopy. Arrows indicate the condensed or fragmented nuclei. Images shown are representative of three independent experiments. C: Percent apoptosis in Annexin V-FITC/PI-stained DU145 cells treated with varying concentrations of carvacrol (0–250 μM) for 24 h observed by flow cytometric analysis. The lower right (LR) quadrant of the histograms indicates the early apoptotic cells, and the upper right (UR) quadrant indicates the late apoptotic cells. Data shown are representative of three independent experiments (D) Percent apoptosis as observed by Annexin V-FITC/PI assay. The results represented are the mean ± SEM of three independent experiments performed in triplicate ($^{*}P < 0.01$, $^{**}P < 0.001$, $^{***}P < 0.0001$ represent significant difference compared with control).

morphology. Similarly, cells with bright-blue fluorescence and condensed nuclei were observed in DU145 cells stained with Hoechst 33342, indicating apoptosis (Fig. 2B). However, there was no significant apoptosis in untreated DU145 cells which showed blue, diffusely stained intact nuclei. The results, ultimately, suggested that carvacrol induced apoptosis in DU145 cells in a dose-dependent manner.

Carvacrol-Induced Apoptosis in Prostate Cancer DU145 Cells

To determine whether the loss of viability in DU145 cells induced by carvacrol was due to apoptosis, DU145 cells were treated with 0–250 μM carvacrol for 24 h and phosphatidylserine (PS) externalization was measured by fluorescence-activated cell sorting (FACS) after Annexin-V FITC/PI staining. Untreated control cells were primarily negative for Annexin V-FITC and PI (LL: viable). Among the treated groups were cells that were Annexin V-FITC positive and PI negative (LR: early apoptotic), Annexin V-FITC and PI positive (UR: late apoptotic) and Annexin V-FITC negative and PI positive (UL: dead or necrotic). As shown in Fig. 2C carvacrol reduced the number of surviving cells and increased the number of both early and late apoptotic cells in a dose-dependent manner. The results showed that carvacrol induced significant amount of apoptosis in DU145 cells of about 9.74%, 15.63%, 19.41%, and 26.44% after 24 h of treatment with 25, 50, 100, and 250 μM of carvacrol respectively (Fig. 2D).

Carvacrol-Induced Caspase Activation in Prostate Cancer DU145 Cells

The downstream signals during apoptosis are transmitted via caspases, a group of cysteine-aspartate proteases, which, upon conversion from pro to active forms, mediate the proteolytic cleavage of many key cellular proteins. Accordingly, we determined whether carvacrol-induced apoptosis in DU145 cells was due to the activation of caspases. Since, caspase-3 is the main downstream effecter caspase in apoptotic pathway, we determined its activity in treated and untreated control. Our results showed a significant induction of caspase-3 activity in DU145 cells after treatment with different concentrations of carvacrol for 24 h (Fig. 3A). Caspase-3 activity was significantly increased as compared to untreated control by 27.53%, 52.60%, and 79.20% at concentrations of 25, 50, and 100 μM carvacrol, respectively. However, caspase-3 activity was dramatically increased to 134.12% at the dose of 250 μM carvacrol (Fig. 3A). Thus, caspase-3 activity in carvacrol-treated DU145 cells was found to be dose-dependent.

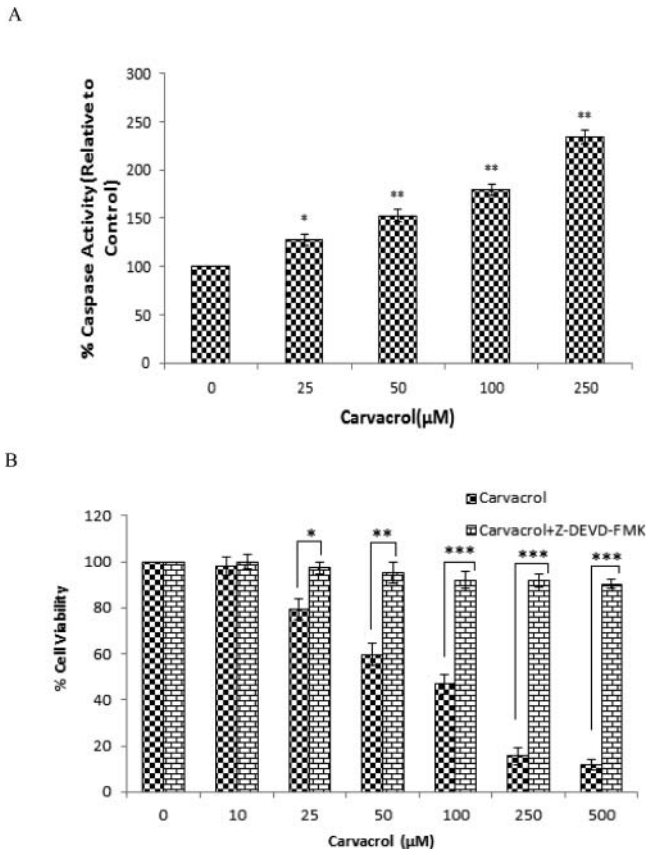

Figure 3. Dose-dependent activation of caspase-3 in carvacrol-treated DU145 cells. A: Percent caspase-3 activity in DU145 cells treated with different concentrations of carvacrol (0–250 μM) for 24 h determined by caspase-3 activity assay. B: Percent cell viability of DU145 cells pretreated with a caspase-3 inhibitor, Z-DEVD-FMK, and then treated with different doses of carvacrol (0–500 μM) for 24 h assessed by MTT assay. Data represent mean ± SEM of three independent experiments performed in triplicate ($^{*}P < 0.01$, $^{**}P < 0.001$, $^{***}P < 0.0001$ represent significant difference compared with control).

Attenuation of Carvacrol-Induced Apoptosis by Caspase-3 Inhibitor

To characterize whether carvacrol-induced cytotoxicity in prostate cancer cells was due to activation of caspase-3, DU145 cells were pretreated with 50 μM Z-DEVD-FMK (a caspase-3 inhibitor) for 2 h and then treated with carvacrol at the indicated concentrations for 24 h. The cell viability was determined using the MTT assay as described above. Pretreatment with capase-3 inhibitor significantly reduced the amount of cytotoxicity in prostate cancer cells caused by the treatment of carvacrol (Fig. 3B). These data

indicated that the induction of caspase-3 activity played a crucial role in carvacrol-induced apoptosis.

Carvacrol Augmented Intracellular ROS Generation in Prostate Cancer Cells

To elucidate the mechanism of action of carvacrol, we further investigated the effect of carvacrol on the intracellular redox status. Accordingly, we determined the intracellular ROS level in carvacrol-treated and untreated prostate cancer cells by measuring the oxidation of non-fluorescent DCFH-DA to its highly fluorescent derivative 2′,7′-dichlorofluorescein (DCF). Briefly, DCFH-DA staining was applied to prostate cancer cells to detect the changes in intracellular ROS level after 12 h of carvacrol treatment. The photomicrograph suggested that carvacrol stimulated ROS formation in DU145 cells in a dose-dependent manner (Fig. 4A). As compared to control cells, carvacrol treatments caused stronger fluorescence intensity in DU145 cells, which indicated an enhanced intracellular ROS levels. Maximum ROS generation was observed in the cells treated at 500 μM carvacrol.

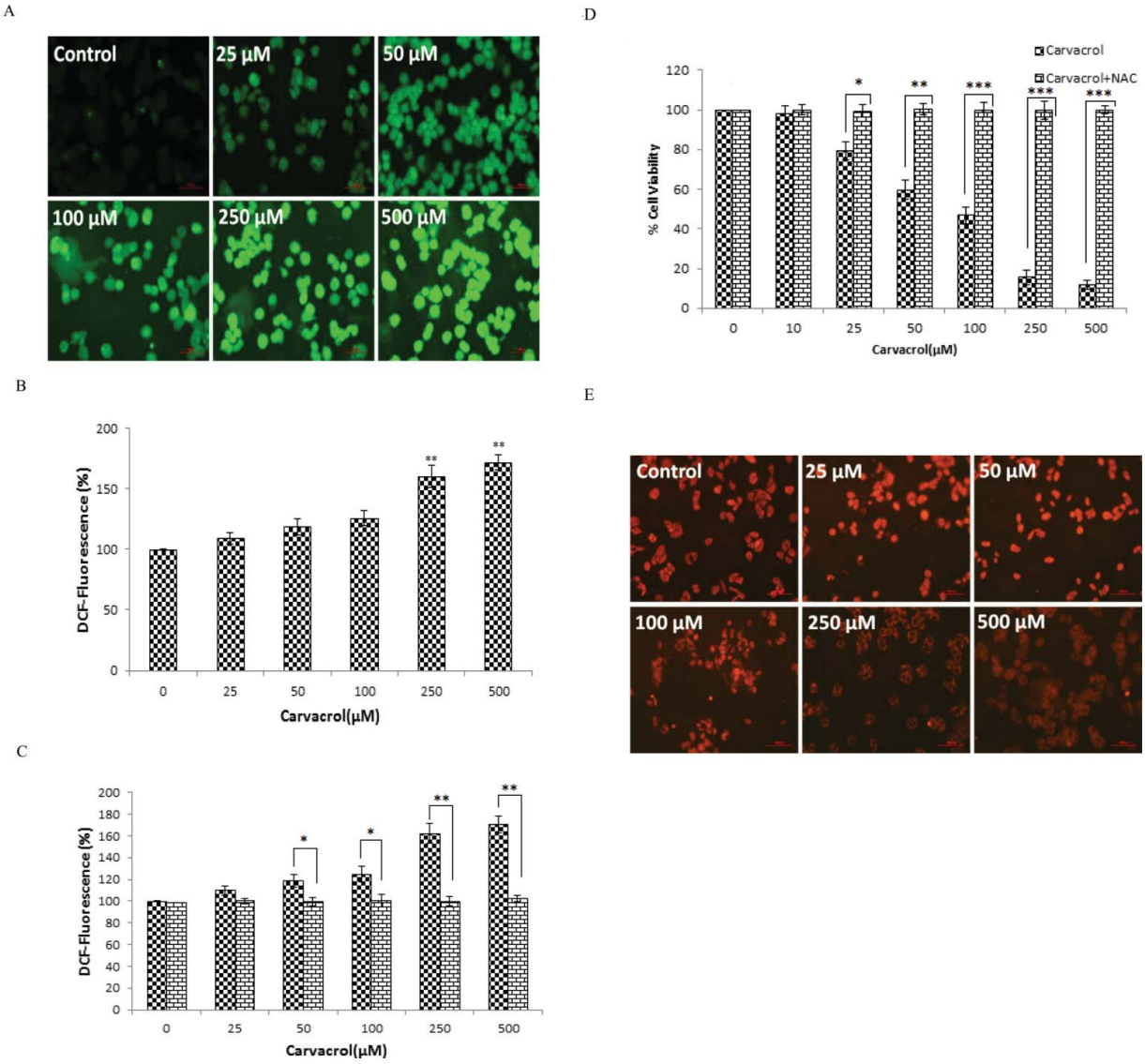

Figure 4. Augmentation of ROS generation in DU145 cells treated with carvacrol. A: Enhanced ROS generation in DCFH-DA stained DU145 cells treated with different concentrations of carvacrol (0–500 μM) analyzed by fluorescence microscopy. Data shown are representative of three independent experiments. B: Quantification of ROS level in terms of percent DCFDA fluorescence in DU145 cells treated with different concentrations of carvacrol (0–500 μM). C: ROS level in DU145 cells pretreated with a ROS inhibitor, NAC and then treated with different doses of carvacrol (0–500 μM). D: Percent cell viability of DU145 cells pretreated with NAC and then treated with different doses of carvacrol (0–500 μM) for 24 h assessed by MTT assay. E: Disruption of the mitochondrial membrane potential ($\Delta\Psi$m) of DU145 cells treated with 0–500 μM of carvacrol observed by staining with a fluorescent dye Rh123. Values are expressed as mean ± SEM of three independent experiments ($^{**}P < 0.01$ and $^{**}P < 0.001$ as compared with control).

The quantitative measurement of ROS intensity showed that 25 μM of carvacrol elevates significant ROS production in DU145 cells, approximately 9.80%, as compared to control. However, ROS production was further augmented to approximately 18.74%, 25.03%, 62.14%, and 70.36% at the concentrations 50, 100, 250, and 500 μM of carvacrol, respectively (Fig. 4B). In order to corroborate the carvacrol-mediated augmentation of ROS level, prostate cancer DU145 cells were pretreated with a known ROS inhibitor, NAC. The quantitative estimation indicated the attenuation of increased ROS level by pretreatment with 10 mM NAC which substantiated our finding that carvacrol could enhance ROS generation in cancer cells (Fig. 4C). Increased ROS generation has been shown to be involved in the induction of apoptosis through various pathways.

Attenuation of Carvacrol-induced Cytotoxicity by N-Acetyl-L-cysteine (NAC)

To further investigate the role of ROS in carvacrol-induced cytotoxicity in prostate cancer cells, we examined the effects of carvacrol in DU145 cells in the presence of NAC (10 mM) by MTT assay. DU145 cells were treated with the ROS scavenger NAC at 10 mM for 2 h and then with carvacrol for an additional 24 h. Pretreatment with ROS inhibitor NAC significantly reduced the amount of cytotoxicity caused by the treatment of carvacrol as evident in Fig. 4D. These data indicated that the augmented intracellular ROS production is critical for the observed carvacrol-induced apoptosis.

Carvacrol Disrupted Mitochondrial Membrane Potential in DU145 Cells

An early event of the intrinsic apoptotic pathway is the damage and loss of mitochondrial membrane potential ($\Delta\Psi$m). To further verify whether carvacrol could disrupt the mitochondrial membrane potential, we used a mitochondria-specific and voltage-dependent dye Rh123 to detect alterations in $\Delta\Psi$m in DU145 cells. After treatment with carvacrol, the fluorescence intensity in cells weakened, indicating a decreased level of $\Delta\Psi$m. As the concentration of carvacrol increased, the level of $\Delta\Psi$m correspondingly decreased (Fig. 4E). Therefore, the result signifies that there is a reduction in the $\Delta\Psi$m of DU145 cell line after treating with carvacrol in a dose-dependent manner.

Carvacrol-Induced Cell Cycle Arrest in Prostate Cancer Cells

To determine whether suppression of cell proliferation by carvacrol results from disruption of cell cycle progression, DU145 cells were treated with 0–500 μM carvacrol for 24 h and subjected to flow cytometry analysis of PI-stained cells. The result showed that carvacrol treatment over 24 h caused a significant cell cycle arrest in DU145 cells at G_0/G_1 phase (Fig. 5A and B). The cell cycle distribution in untreated control was 37.12%, 14.19%, and 48.68% for G_0/G_1, G_2/M, and S phase, respectively. The treatment with lower dose (25 μM) carvacrol resulted in the reduction of S and G_2/M phase cell population and increase in G_0/G_1 phase population (Fig. 5A). A further increase in carvacrol concentration to 50, 100, and 250 μM resulted in a more pronounced reduction of cells in S phase with a concomitant accumulation of cells in G_0/G_1 phase (Fig. 5B). The G_0/G_1 phase cell cycle distribution for DU145 cells was 44.21%, 48.09%, 55.29%, and 62.39% at the dose of 25, 50,100, and 250 μM of carvacrol, respectively (Fig. 5B). The increase in G_0/G_1 phase cell population was accompanied by a simultaneous decrease in the S phase cell population which was found to be 45.56%, 42.99%, 34.32%,

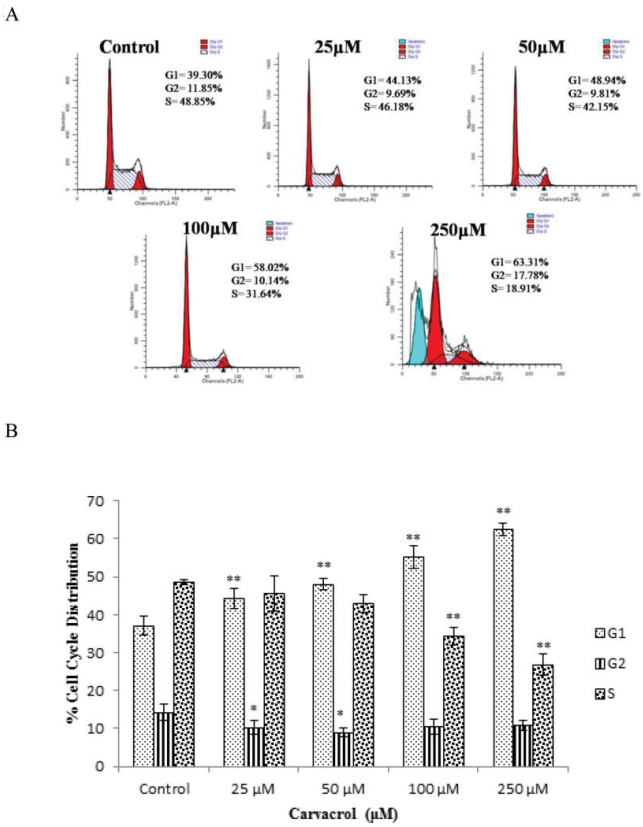

Figure 5. Carvacrol induced cell cycle arrest in a dose-dependent manner. A: Cell cycle distribution of propidium iodide-stained DU145 cells treated with 0–250 μM carvacrol for 24 h observed by flow cytometric analysis. The data shown here are from a representative experiment repeated three times. B: Percent cell cycle distributions determined by flow cytometric analysis. Data represent mean ± SEM of three independent experiments performed in triplicate ($^{*}P < 0.05$ and $^{**}P < 0.01$ as compared to control).

and 26.87% at the concentration of 25, 50,100, and 250 μM of carvacrol, respectively.

Discussion

Prostate cancer remains the leading cause of death in males largely because of late-stage diagnosis and limited effective treatments, especially in the recurrent disease (38). Many natural dietary substances have been found to have significant anticancer potential due to their ability to inhibit tumor growth, angiogenesis, and metastasis without much side effects and thus, could be an important avenue aiming to reduce both the incidence and the mortality of cancer by preventing, reversing, or delaying the process of carcinogenesis (39–42). Carvacrol is one of the compounds found in essential oils of oregano and thyme. Carvacrol has been reported to exhibit antiproliferative and anticancer activities in a few recent preliminary studies (24–28). Therefore, we explored the mode of action and potential utility of carvacrol in prostate cancer cells in the quest of finding a novel, effective anticancer agent.

In the current study, we attempted to delineate the effects of the carvacrol on prostate cancer DU145 cell line. The cell viability analysis by MTT assay and trypan blue dye exclusion assay suggested that carvacrol strongly inhibited the proliferation of prostate cancer cells (Fig. 1B and C). Furthermore, morphological analysis by phase contrast microscopy showed that shapes of the cells were significantly changed, being round in the carvacrol-treated groups which was characterized by cellular shrinkage and detached from surface, forming clusters (Fig. 1D and E). These results suggested that the treatment of carvacrol significantly reduced the cell viability of prostate cancer cells in a dose-dependent manner. We did not observe significant cytotoxicity in normal mouse macrophages after carvacrol treatment; however, a substantial effect on cell viability was observed only at the highest concentration of carvacrol used in the experiment. Thus, carvacrol was shown to exert cytotoxic effects in human prostate cancer cells without incurring significant cytotoxic effect on normal cells. Results from previous studies have shown similar effects of carvacrol on different cancer cells (22–28).

Preceding reports have indicated that most of the chemotherapeutic agents reduce cancer cell proliferation by inducing apoptosis (43). Morphological hallmarks of apoptosis are chromatin condensation and nuclear fragmentation, which are accompanied by rounding up of the cell, reduction in cellular volume (pyknosis), and formation of apoptotic bodies (44,45). Our results also support the above notion where fragmented and condensed nuclei stained with DAPI and Hoechst 33342 in DU145 cells suggested that carvacrol induced apoptosis in prostate cancer cells (Fig. 2A and B). We further characterized the cytotoxicity of carvacrol by examining the presentation of the early apoptotic marker phosphatidylserine at the cell surface by FITC-Annexin V assay. In apoptotic cells, the membrane phospholipid phosphatidylserine (PS) is translocated from the inner to the outer leaflet of the plasma membrane by flip-flop movement, thereby exposing PS to the external cellular environment (46). Annexin V is a 35–36 kDa Ca^{2+}-dependent phospholipid-binding protein that interacts specifically with phosphatidylserine and can be used for the detection of apoptosis. As shown in Fig. 2C and D, results of FITC-Annexin V assay demonstrated a dose-dependent increase in the Annexin V positive cells, indicating the induction of apoptosis in DU145 prostate cancer cells by carvacrol. This finding was in accordance with the previously reported studies (24–28).

Caspases are synthesized as inactive proenzymes and their activation during apoptosis results in cleavage at specific aspartate cleavage sites (47,48). While initiator caspases-8 and -9 undergo autocatalytic activation, executioner pro-caspase-3 is processed by initiator caspases. Caspase-3 is one of the key executioners of apoptosis, being responsible either partially or totally for the proteolytic cleavage of many cellular proteins (49,50). We, therefore, investigated caspase activity in treated and untreated cells and observed that carvacrol induced caspase-3 activation, leading to apoptosis (Fig. 3A and B). Pretreatment with capase-3 inhibitor substantially reduced carvacrol-induced cytotoxicity in prostate cancer cells, indicating activation of caspase-3 during carvacrol-induced apoptosis (Fig. 3A and B). This result was also in agreement with the earlier reports of carvacrol (24–28).

Cancer cells produce high levels of ROS that lead to a state of increased basal oxidative stress. Since this state of oxidative stress makes cancer cells vulnerable to agents that further augment ROS levels, the use of pro-oxidant agents is emerging as an exciting strategy to selectively target tumor cells (51). However, the induction of ROS formation plays an important role in the chemotherapeutic activity of several anticancer drugs and a large number of anticancer compounds (52,53). Our data for the qualitative and quantitative analysis of ROS generation suggested that carvacrol induced ROS-mediated induction of apoptosis in DU145 cells in a concentration-dependent manner (Fig. 4A and B). However, the carvacrol-mediated augmentation of ROS levels in prostate cancer cells were attenuated by pretreatment of cells with a ROS inhibitor, NAC (Fig. 4C). Furthermore, pretreatment with NAC significantly reduced the amount of cytotoxicity caused by the treatment of carvacrol

(Fig. 4D). These data indicated that the augmented intracellular ROS production is critical for the observed carvacrol-induced apoptosis which has not been reported previously in any studies.

Disruption of mitochondrial membrane potential ($\Delta\Psi m$) has been proposed as an important prerequisite in the activation of apoptosis (54,55). Rhodamine123, a cationic fluorescent dye whose mitochondrial fluorescence intensity decreases quantitatively in response to dissipation of mitochondrial transmembrane potential, has been used previously to evaluate disturbances in mitochondrial membrane potential (56). Our results also supported the above fact that carvacrol depolarized the mitochondrial membrane potential ($\Delta\Psi m$) significantly in a dose-dependent manner (Fig. 4E) (57,58). Carvacrol-mediated disruption of mitochondrial membrane potential ($\Delta\Psi m$), which could be the probable mode of action of carvacrol, has also not been reported in earlier reports.

It is well known that carcinogenesis is closely associated with uncontrolled cell cycle. In order to elucidate the type of death induced by carvacrol, the percentage of cells in the sub-G_1 (apoptosis), G_0/G_1, S, andG_2/M phases was determined by flow cytometry using PI staining. G_1 and G_2 phases of the cell cycle are the major check points and have an important role in cell cycle progression. Through cell cycle analysis, we observed an interesting phenomenon that carvacrol arrested cell cycle progression in G_0/G_1 by blocking the transition from G_1 to S phase and consequently lead to apoptosis (Fig. 5A and B) (26). Thus, we are reporting for the first time that apart from inducing apoptosis, carvacrol could also induce cell cycle arrest in prostate cancer cells.

Conclusion

In conclusion, the present study provides insight into the mechanism of antiproliferative and apoptotic action of carvacrol against human prostate cancer cells. The results shows a link between antiproliferative and apoptotic induction, and the cell death in prostate cancer cells was due to the induction of ROS-mediated mitochondrial membrane depolarization and caspase activation. We also observed that carvacrol induced cell cycle arrest in prostate cancer cells. Thus, our data confirmed the potential of carvacrol as a chemopreventive agent in human prostate cancer cells, and therefore, may be potentially valuable for application in drug developments. Further studies are underway to elucidate the molecular mechanisms involved to prove efficacy of carvacrol as an anticancer agent against prostate cancer cells.

Acknowledgment

The authors thank the management of Integral University for providing the facilities to carry out this study. The manuscript has manuscript id provided by Research and Development office, Integral University, Lucknow (IU/R&D/2017-1 MCN 00010).

Declaration of Interest

I confirm that this research paper authored by me/us is an original and genuine research work. It has neither been submitted for publication nor published elsewhere in any print/electronic form.

References

1. Ferlay J, Shin HR, Bray F, Forman D, Mathers C, et al.: GLOBOCAN 2008 v1.2, Cancer Incidence and Mortality Worldwide2010: IARC Cancer Base No. 10 [http://globocan.iarc.fr/]. Lyon, France: International Agency for Research on Cancer. Available from: http://globocan.iarc.fr, accessed on 03/11/2012.
2. Beaulieu N, Bloom D, Bloom R, and Stein R. *Breakaway: The Global Burden of Cancer—Challenges and Opportunities*. London, UK: The Economist Intelligence Unit, 2009.
3. Lalitha K, Suman G, Pruthvish S, Mathew A, and Murthy NS: Estimation of time trends of incidence of prostate cancer—an Indian scenario. *Asian Pacific J Cancer Prev* **13** (12), 6245–6250, 2012.
4. Jain S, Saxena S, and Kumar A: Epidemiology of prostate cancer in India. *Meta Gene* **2**, 596–605, 2014.
5. National Cancer Registry Programme (NCRP). Time trends in Cancer Incidence rates 1982–2005, Indian Council of Medical Research, Bangalore, India, 2009.
6. Clinton SK and Giovannucci E: Diet, nutrition and prostate cancer. *Annu Rev Nutr* **18**, 413–440, 1998.
7. Abdulla M and Gruber P: Role of diet modification in cancer prevention. *Biofactors* **12**, 45–51, 2000.
8. Gordaliza M: Natural products as leads to anticancer drugs. *Clin Transl Oncol* **9**, 67–776, 2007.
9. Bommareddy A, Eggleston W, Prelewicz S, Antal A, Witczak Z, et al.: Chemoprevention of prostate cancer by major dietary phytochemicals. *Anticancer Res* **33**, 4163–4174, 2013.
10. Kumar N and Chornokur G: Molecular targeted therapies using botanicals for prostate cancer chemoprevention. *Transl Med* **S2**, 005, 2012.
11. Yu H, Zhang ZI, Chen J, Pei A, Hua F, et al.: Carvacrol, a food-additive, provides neuroprotection on focal cerebral ischemia/reperfusion injury in mice. *PLoS One* **7**, e33584, 2012.
12. Martins RRL, Neves MG, Sivestre AJD, Silva A, and Cavaleiro JAS: Oxidation of aromatic monoterpene with hydrogen peroxide catalyzed by Mn(III) porphyrin complexes. *J Molcatal A: Chem* **137**, 41–47, 1999.
13. Aligiannis N, Kalpoutzakis E, Mitaku S, and Chinou IB: Composition and antimicrobial activity of essential oils of two *Origanum* species. *J Agric Food Chem* **49**, 4168–4170, 2001.

14. Arcila Lozano CC: Oregano: properties, composition and biological activity. *Arch Latinoam Nut* **54**, 100–111, 2004.
15. Sokmen M, Serkedjieva J, Daferera D, Gulluce M, Polissiou M, et al.: In vitro antioxidant, antimicrobial and antiviral activities of the essential oil and various extract from herbal parts and callus cultures of *Origanum acutidens*. *J agric Food Chem* **52**, 3309–3312, 2004.
16. Kisk G and Roller S: Carvacrol and p-cymene inactivate Escherichia coli O157:H7 in apple juice. *BMC Microbiol* **5**, 36, 2005.
17. Lampronti I, Saab AM, and Gambari R: Antiproliferative activity of essential oils derived from plants belonging to the Magnoliophyta division. *Int J Oncol* **29**, 989–995, 2006.
18. Horvathova E, Turcanniova V, and Slamenova D: Comparative study of DNA-damaging and DNA-protective effects of selected components of essential plant oils in human leukemic cells K562. *Neoplasma* **54**, 478–483, 2007.
19. Baser KHC: Biological and pharmacological activities of carvacrol and carvacrol bearing essential oils. *Curr Pharm Des* **14**, 3106–3119, 2008.
20. Gany ZSA and Mahdi MF: Cytotoxic assay of *Nigella sativa* leaf callus extract (thymol) on hep-3 cell line using ELISA assay. *Iraqi J Pharma Sci* **17**, 63–67, 2008.
21. Giweli A, Dz'amic' AM, Sokovic' M, Ristic' MS, and Marin PD: Antimicrobial and antioxidant activities of essential oils of *Satureja thymbra* growing wild in Libya. *Molecules* **17**, 4836–4850, 2012.
22. Koparal AT and Zeytinoglu M: Effects of carvacrol on a human non-small cell lung cancer (NSCLC) cell line, A549. *Cytotechnology* **43**, 149–154, 2003.
23. Karkabounas S, Kostoula OK, Daskalou T, Veltsistas P, Karamouzis M, et al.: Anticarcinogenic and antiplatelet effects of carvacrol. *Exp Oncol* **28**, 121–125, 2006.
24. Arunasree KM: Anti-proliferative effects of carvacrol on a human metastatic breast cancer cell line, MDA-MB 231. *Phytomedicine* **17**, 581–588, 2010.
25. Mehdi SJ, Ahmad A, Irshad M, Manzoor N, and Rizvi MMA: Cytotoxic effect of Carvacrol on human cervical cancer cells. *Biol Med* **3**(2), 307–312, 2011.
26. Yin QH, Yan FX, Zu XY, Wu YH, Wu XP, et al.: Anti-proliferative and pro-apoptotic effect of carvacrol on human hepatocellular carcinoma cell line HepG-2. *Cytotechnology* **64**, 43–51, 2012.
27. Patel B, Shah VR, and Bavadekar SA: Anti-proliferative effects of carvacrol on human prostate cancer cell line, LNCaP. *FASEB J* **26**, 1037.5, 2012.
28. Ahmed, Shousha WG, El-Mezayen HA, Ismaiel NN, and Mahmoud NS: *In vivo* antitumor potential of carvacrol against hepatocellular carcinoma in rat model. *World J Pharm Pharm Sci* **2**, 2367–2396, 2013.
29. Yang CB, Pei WJ, Zhao J, Yuan-yuan Cheng YY, et al.: Bornyl-caffeate induces apoptosis in human breast cancer MCF-7 cells via the ROS- and JNK-mediated pathways. *Acta Pharmacol Sin* **35**(1), 113–123, 2013.
30. Prasad R and Katiyar SK: Bioactive phytochemical proanthocyanidins inhibit growth of head and neck squamous cell carcinoma cells by targeting multiple signaling molecules. *PLoS One* **7**(9), e46404, 2012.
31. Das S, Dey KK, Dey G, Pal I, Majumder A, et al.: Antineoplastic and apoptotic potential of traditional medicines thymoquinone and diosgenin in squamous cell carcinoma. *PLoS One* **7**(10), e46641, 2012.
32. Ahamad MS, Siddiqui S, Jafri A, Ahmad S, Afzal M, et al.: Induction of apoptosis and antiproliferative activity of naringenin in human epidermoid carcinoma cell through ROS generation and cell cycle arrest. *PLoS One* **9**(10), e110003, 2014.
33. Xiong Y, Ye T, Wang M, Xia Y, Wang N, et al.: A novel cinnamide YLT26 induces breast cancer cells apoptosis via ROS mitochondrial apoptotic pathway in vitro and inhibits lung metastasis in vivo. *Cell Physiol Biochem* **34**, 1863–1876, 2014.
34. Qi H, Siu SO, Chen Y, Han Y, Chu IK, et al.: Senkyunolides reduce hydrogen peroxide-induced oxidative damage in human liver HepG2 cells via induction of heme oxygenase-1. *Chem Biol Interact* **183**, 380–389, 2010.
35. Qi H, Chen B, Le XC, and Rong J: Concomitant induction of heme Oxygenase-1 attenuates the cytotoxicity of arsenic species from lumbricus extract in human liver HepG2 cells. *Chem Biodivers* **9**, 739–754, 2012.
36. Mishra T, Arya RK, Meena S, Joshi P, Pal M, et al.: Isolation, characterization and anticancer potential of cytotoxic triterpenes from *Betula utilis* bark. *PLoS One* **11**(7), e0159430, 2016.
37. Sarkar S, Mazumdar A, Dash R, Sarkar D, Fisher PB, et al.: ZD6474, adual tyrosine kinase inhibitor of EGFR and VEGFR-2, inhibits MAPK/ERKand AKT/PI3-K and induces apoptosis in breast cancer cells. *Cancer Biol Ther* **9**(8), 592–603, 2010.
38. Krishna Moorthy H and Venugopal P: Strategies for prostate cancer prevention—review of the literature. *Indian J Urol* **24**, 295–302, 2008.
39. Donaldson MS: Nutrition and cancer: a review of the evidence for an anti-cancer diet. *Nutr J* **3**, 19, 2004.
40. Shukla S and Gupta S: Dietary agents in the chemoprevention of prostate cancer. *Nutr Cancer* **53**(1), 18–32, 2005.
41. Melchini A, Traka MH, Catania S, Miceli N, Taviano MF, et al.: Antiproliferative activity of the dietary isothiocyanate erucin, a bioactive compound from cruciferous vegetables, on human prostate cancer cells. *Nutr Cancer* **65**(1), 132–138, 2013.
42. Lall RK, Syed DN, Adhami VM, Khan MI, and Mukhtar H: Dietary polyphenols in prevention and treatment of prostate cancer. *Int J Mol Sci* **16**, 3350–3376, 2015.
43. Teiten MH, Gaascht F, Dicato M, and Diederich M: Anticancer bioactivity of compounds from medicinal plants used in European medieval traditions. *Biochem Pharmacol* **86**(9), 1239–1247, 2013. doi: 10.1016/j.bcp.2013.08.007
44. Kroemer G, El-Deiry WS, Golstein P, Peter ME, Vaux D, et al.: Classification of cell death: recommendations of the Nomenclature Committee on Cell Death. *Cell Death Differ* **12**, 1463–1467, 2005.
45. Wong RSY: Apoptosis in cancer: from pathogenesis to treatment. *J Exp Clin Cancer Res* **30**, 87, 2011.
46. Bratton DL, Fadok VA, Richter DA, Kailey JM, Guthrie LA, et al.: Appearance of phosphatidylserine on apoptotic cells requires calcium mediated nonspecific flip-flop and is enhanced by loss of the amino phospholipid translocase. *J Biol Chem* **272**, 26159–26165, 1997.
47. Cohen GM: Caspases: the executioners of apoptosis. *Biochem J* **326**(1), 1–16, 1997.
48. Thornberry NA, Rano TA, Peterson EP, Rasper DM, Timkey T, et al.: A combinatorial approach defines specificities of members of the caspase family and granzyme B.

Functional relationships established for key mediators of apoptosis. *J Biol Chem* **272**, 17907–17911, 1997.
49. Enari M, Sakahira H, Yokoyama H, Okawa K, Iwamatsu A, et al.: A caspase-activated DNase that degrades DNA during apoptosis, and its inhibitor ICAD. *Nature* **391**, 43–50, 1998.
50. Nagata S: Apoptotic DNA fragmentation. *Exp Cell Res* **256**, 12–18, 2000.
51. Cordero CM, González AJL, Montaño JMC, Morón EB, and Lázaro ML: Pro-oxidant natural products as anticancer agents. *Curr Drug Targets* **13**, 1006–1028, 2012.
52. Fruehauf JP and Meyskens FL: Reactive oxygen species: a breath of life or death? *Clin Cancer Res* **13**, 789–794, 2007.
53. Trachootham D, Alexandre J, and Huang P: Targeting cancer cells by ROS mediated mechanisms: a radical therapeutic approach? *Nat Rev Drug Disc* **8**, 579–591, 2009.
54. Scaduto Jr RC and Grotyohann LW: Measurement of mitochondrial membrane potential using fluorescent rhodamine derivatives. *Biophys J* **76**, 469–477, 1999.
55. Balaban R: Modeling mitochondrial function. *Am J Physiol Cell Physiol* **291**, C1107–C1113, 2006.
56. Emaus RK, Grunwald R, and Lemasters JJ: Rhodamine-123 as a probe of transmembrane potential in isolated rat-liver mitochondria-spectral and metabolic properties. *Biochim Biophys Acta* **850**, 436–448, 1986.
57. Polla BS, Kantengwa S, Francois D, Salvioli S, Franceschit C, et al.: Mitochondria are selective targets for the protective effects of heat shock against oxidative injury. *Proc Natl Acad Sci USA* **93**, 6458–6463, 1996.
58. Duan J, Yin Y, Wei G, Cui J, Zhang E, et al.: Chikusetsu saponin IVa confers cardioprotection via SIRT1/ERK1/2and Homer1a pathway. *Sci Rep* **5**, 18123, 2015.